Equivalence of particle-particle random phase approximation correlation energy and ladder-coupled-cluster doubles

Degao Peng, Stephan N. Steinmann, Helen van Aggelen, and Weitao Yang

Citation: The Journal of Chemical Physics **139**, 104112 (2013);
View online: https://doi.org/10.1063/1.4820556
View Table of Contents: http://aip.scitation.org/toc/jcp/139/10
Published by the American Institute of Physics

THE JOURNAL OF CHEMICAL PHYSICS **139**, 104112 (2013)

Equivalence of particle-particle random phase approximation correlation energy and ladder-coupled-cluster doubles

Degao Peng,[1] Stephan N. Steinmann,[1] Helen van Aggelen,[1,2] and Weitao Yang[1,3,a)]
[1]*Department of Chemistry, Duke University, Durham, North Carolina 27708, USA*
[2]*Department of Inorganic and Physical Chemistry, Ghent University, 9000 Ghent, Belgium*
[3]*Department of Physics, Duke University, Durham, North Carolina 27708, USA*

(Received 21 June 2013; accepted 20 August 2013; published online 12 September 2013)

The recent proposal to determine the (exact) correlation energy based on pairing matrix fluctuations by van Aggelen *et al.* ["Exchange-correlation energy from pairing matrix fluctuation and the particle-particle random phase approximation," preprint arXiv:1306.4957 (2013)] revived the interest in the simplest approximation along this path: the particle-particle random phase approximation (pp-RPA). In this paper, we present an analytical connection and numerical demonstrations of the equivalence of the correlation energy from pp-RPA and ladder-coupled-cluster doubles. These two theories reduce to identical algebraic matrix equations and correlation energy expressions. The numerical examples illustrate that the correlation energy missed by pp-RPA in comparison with coupled-cluster singles and doubles is largely canceled out when considering reaction energies. This theoretical connection will be beneficial to design density functionals with strong ties to coupled-cluster theories and to study molecular properties at the pp-RPA level relying on well established coupled cluster techniques. [http://dx.doi.org/10.1063/1.4820556]

I. INTRODUCTION

The random phase approximation (RPA) was originally proposed in the 1950s by Pines and Bohm[1,2] to treat the homogeneous electron gas. Since then, the idea of RPA has spawned the studies of excitation energies, linear-response functions, and correlation energies in solid state physics,[3–6] nuclear physics,[7–12] and quantum chemistry.[13–16] In the recent decade, there has been a renaissance of interest in the RPA correlation energy in quantum chemistry because of its good description of van der Waals interaction,[16] the correct dissociation limit of H_2,[17] and, through the adiabatic connection, its link to density-functional theory (DFT).[16] These features have motivated the development of efficient implementations leading to relatively low scaling algorithms ($O(N^4 \log N)$ by Eshuis and Furche[18] and $O(N^4)$ by Ren *et al.*[19] with N the number of basis functions), and going beyond RPA is an active field of research that achieves exciting results.[20–26]

Recently, van Aggelen *et al.*[27] established an adiabatic connection for the exchange-correlation energy in terms of the dynamic paring matrix fluctuation, parallel to the adiabatic connection fluctuation dissipation (ACFD) theorem in terms of the density fluctuation.[5,28] Like the ACFD theorem, this adiabatic connection is in principle exact, but requires the particle-particle propagator as a function of the interaction strength. The particle-particle channel of random phase approximation (pp-RPA) is the first-order approximation to the paring matrix fluctuation. The preliminary applications of the pp-RPA correlation energies to molecular systems provide promising results in describing systems with both fractional charge and fractional spin.[27] The RPA usually applied in quantum chemistry describes exclusively the particle-hole channel of correlations. To distinguish the two RPAs of different channels, we will, hereafter, refer to the conventional particle-hole RPA as ph-RPA. In nuclear physics, pp-RPA,[7,8,29–37] also known as Brueckner's theory,[38–41] is also widely discussed. Except for computational studies of Auger spectroscopy,[42,43,82] pp-RPA has not been applied in chemistry before the development of van Aggelen *et al.*[27]

In the diagrammatic language extensively used in many-body perturbation-theory (MBPT), the ph-RPA correlation energy is the sum of all ring diagrams.[7,44] Čížek[45] exploited the same diagrammatic arguments in his seminal work and identified ph-RPA as a subset of the coupled-cluster doubles (CCD) equations, i.e., accounting only for the ring summation terms. The ph-RPA wavefunction being of an exponential form is textbook knowledge.[8] Despite the well-known equivalence between the ph-RPA correlation energy and summation of all ring diagrams in direct ring-CCD, the mathematical connection between the linear ph-RPA equation and the quadratic equation in direct ring-CCD has only recently been presented by Scuseria *et al.*,[46] while ideas can be traced back to work done forty years before.[47] On the other hand, the pp-RPA correlation energy can be interpreted as the sum of all ladder diagrams.[7] As the sum of all ladder diagrams, methods like pp-RPA have also been closely related to the "ladder approximation" in the literature.[48] Again, considering the diagrams involved, Čížek identified the sum of all ladder diagrams as a subset of CCD, which might be called ladder-CCD,[45] and the exponential form of the pp-RPA wavefunction is also found in textbooks.[8] However, the authors are not aware of any explicit demonstration of the equivalence of the linear form of the pp-RPA equation and the quadratic ladder-CCD equation. The purpose of this paper is, following

a)Electronic mail: weitao.yang@duke.edu

Ref. 46, to establish this connection between the two sets of seemingly distinct equations. Since pp-RPA is a straightforward approximation in Green's function theory,[27] the establishment of this connection might shed light on the relationship between Green's function based methods and coupled-cluster theory, a perspective from which both fields could benefit. Furthermore, it is the authors' hope that the insight gained from linking Green's functions, coupled-cluster theory, and DFT provides new stimulus to develop novel density functional approximations. Moreover, the coupled-cluster connection opens up a direct way to obtain molecular properties from a virtual orbital dependent density functional, and the pp-RPA based excited states can straightforwardly be obtained via equation-of-motion coupled-cluster[49–52] or linear-response coupled-cluster theory.[53,54]

II. THE PP-RPA EQUATION AND ITS STABILITY

The pp-RPA equation can be derived from the two-particle Green's function, the equation-of-motion ansatz, or the linear-response time-dependent Hartree-Fock-Bogoliubov approximation (TDHFB).[7,8,27,33] The resulting generalized eigenvalue equation is very similar to the ph-RPA equation (see, for example, Refs. 7, 8, 16, and 46 for the ph-RPA equation),

$$\begin{bmatrix} \mathbf{A} & \mathbf{B} \\ \mathbf{B}^\dagger & \mathbf{C} \end{bmatrix} \begin{bmatrix} \mathbf{x}_n \\ \mathbf{y}_n \end{bmatrix} = \omega_n \begin{bmatrix} \mathbf{I} & \mathbf{0} \\ \mathbf{0} & -\mathbf{I} \end{bmatrix} \begin{bmatrix} \mathbf{x}_n \\ \mathbf{y}_n \end{bmatrix}, \tag{1}$$

where

$$A_{ab,cd} = (\epsilon_c + \epsilon_d - 2\nu)\delta_{ac}\delta_{bd} + \langle ab||cd\rangle, \tag{2}$$

$$C_{ij,kl} = -(\epsilon_k + \epsilon_l - 2\nu)\delta_{ki}\delta_{jl} + \langle ij||kl\rangle, \tag{3}$$

and

$$B_{ab,ij} = \langle ab||ij\rangle. \tag{4}$$

We use indexes $i, j, k, l\ldots$ for occupied spin orbitals (holes), $a, b, c, d\ldots$ for unoccupied spin orbitals (particles), and u, v, $s, t\ldots$ for general spin orbitals. Furthermore, m, n are used to denote eigenvector and eigenvalue indexes. Additionally, ϵ_u is the molecular orbital eigenvalue, and $\langle uv||st\rangle$ is the antisymmetrized two-electron integral

$$\langle uv||st\rangle = \langle uv|st\rangle - \langle uv|ts\rangle, \tag{5}$$

where

$$\langle uv|st\rangle = \sum_{\sigma_1\sigma_2}\int d\mathbf{r}_1 d\mathbf{r}_2 \frac{\phi_u^*(\mathbf{r}_1\sigma_1)\phi_v^*(\mathbf{r}_2\sigma_2)\phi_s(\mathbf{r}_1\sigma_1)\phi_t(\mathbf{r}_2\sigma_2)}{|\mathbf{r}_1 - \mathbf{r}_2|}. \tag{6}$$

The chemical potential ν is not a necessity in the equation-of-motion[8,33] or the two-particle Green's function derivation;[27] however, during the derivation from the TDHFB,[7] ν is used to ensure that the ground state has the desired number of electrons N. In practice, it is usually approximated to be half of HOMO (highest occupied molecular orbital) and LUMO (lowest unoccupied molecular orbital) eigenvalues.[27] We will later show that the exact choice of the chemical potential is unimportant within a certain range as long as the pp-RPA equation is stable.

The indexes of the matrix are either hole pairs or particle pairs. These indexes have only $i > j$ for hole pairs and $a > b$ for particle pairs to eliminate the redundancy. The number of particle (hole) pairs is

$$N_{pp(hh)} = \frac{1}{2}N_{\text{vir(occ)}}(N_{\text{vir(occ)}} - 1), \tag{7}$$

where $N_{\text{vir(occ)}}$ is the number of virtual (occupied) orbitals. In general, N_{pp} is much larger than N_{hh}. The upper left (lower right) identity matrix in Eq. (1) has the same dimension as $\mathbf{A}$ ($\mathbf{C}$). Throughout the paper, the dimensions of identity matrices will be omitted, as they are clear from the context. The difference of the dimensions of $\mathbf{A}$ and $\mathbf{C}$ makes the solution of the pp-RPA equation quite different from that of the usual ph-RPA equation or the linear-response time-dependent DFT equation.[55] Nevertheless, Eq. (1) and the ph-RPA equation share conceptually similar properties as discussed in Ref. 10.

For simplicity, we use a compact matrix notation

$$\mathbf{M}\mathbf{z}_n = \omega_n \mathbf{W}\mathbf{z}_n, \tag{8}$$

to denote Eq. (1), where $\mathbf{M}$ is the Hermitian matrix on the left-hand side

$$\mathbf{M} = \begin{bmatrix} \mathbf{A} & \mathbf{B} \\ \mathbf{B}^\dagger & \mathbf{C} \end{bmatrix}, \tag{9}$$

$\mathbf{W}$ is the non-positive definite metric

$$\mathbf{W} = \begin{bmatrix} \mathbf{I} & \mathbf{0} \\ \mathbf{0} & -\mathbf{I} \end{bmatrix}, \tag{10}$$

and $\mathbf{z}_n$ is the full eigenvector

$$\mathbf{z}_n = \begin{bmatrix} \mathbf{x}_n \\ \mathbf{y}_n \end{bmatrix}, \tag{11}$$

with its eigenvalue ω_n. Due to the non-positive definite metric $\mathbf{W}$, Eq. (1) is not guaranteed to have all real eigenvalues. We call $\mathbf{z}_n^\dagger \mathbf{W}\mathbf{z}_n$ the signature of an eigenvector $\mathbf{z}_n$. The signature can be positive, zero, or negative. The zero signature coincides with an imaginary eigenvalue (see Subsection 1 in the Appendix), while positive and negative signatures are associated with real eigenvalues. We categorize the eigenvectors according to their signatures, where eigenvectors with positive signatures are called $N + 2$ excitations and eigenvectors with negative signatures are called $N - 2$ excitations. For a diagonalizable pp-RPA equation with all real eigenvalues, according to Subsection 2 in the Appendix, the orthonormalization of the eigenvectors can be written as

$$\mathbf{Z}^\dagger \mathbf{W}\mathbf{Z} = \mathbf{W}, \tag{12}$$

with all $N+2$ eigenvectors to the left of all $N-2$ eigenvectors in $\mathbf{Z}$. This special arrangement will be kept all through the paper.

When all the eigenvalues of a diagonalizable pp-RPA equation are real, the pp-RPA equation is defined to be stable if all the $N + 2$ excitation eigenvalues are positive and $N - 2$ excitation eigenvalues are negative, i.e., $\min_n \omega_n^{N+2} > 0 > \max_m \omega_m^{N-2}$. With the eigenvector arrangement according to signatures, the stability condition can be expressed in a concise equation,

$$\mathrm{sign}(\boldsymbol{\omega}) = \mathbf{W}, \tag{13}$$

where $\mathrm{sign}(\boldsymbol{\omega})$ is the sign function[56] of the eigenvalue matrix $\boldsymbol{\omega}$, which gives $[\mathrm{sign}(\boldsymbol{\omega})]_{nm} = \delta_{nm}\mathrm{sign}(\omega_n)$, since $\boldsymbol{\omega}$ is diagonal. Note that Eq. (12) is a necessary but not sufficient condition for the stability of Eq. (13).

These eigenvalues are interpreted as the double ionization and double electron attachment energies in a molecular system, i.e.,

$$\omega_n^{N+2} = E_n^{N+2} - E_0^N - 2\nu \tag{14}$$

are the $N+2$ excitation energies, and

$$\omega_n^{N-2} = E_0^N - E_n^{N-2} - 2\nu \tag{15}$$

are the $N-2$ excitation energies. With the eigenvalue interpretation of Eqs. (14) and (15), an unstable pp-RPA equation violates the energy convexity condition.[57] It has not been proved that such stability is intrinsic for a self-consistent solution of a Hartree-Fock or Kohn-Sham/generalized Kohn-Sham molecular system, but in practice unstable solutions have never been encountered for molecular systems so far in Ref. 27 and in present work, as compared to the notorious instability issue of ph-RPA with exchange, namely, the Hartree-Fock instability.[10,58,59]

The stability condition of the pp-RPA equation is equivalent to the positive definiteness of the matrix $\mathbf{M}$ (see Subsection 3 in the Appendix and Ref. 7 for further details).

With the whole spectrum of a stable pp-RPA equation, the pp-RPA correlation energy can be expressed in several equivalent ways:[27]

$$E_c^{\text{pp-RPA}} = \sum_m \omega_m^{N+2} - \mathrm{Tr}\mathbf{A} = -\sum_n \omega_n^{N-2} - \mathrm{Tr}\mathbf{C}$$
$$= \frac{1}{2}\sum_n |\omega_n| - \frac{1}{2}\mathrm{Tr}\mathbf{M}. \tag{16}$$

The precise value of ν is irrelevant for the correlation energy, since it cancels out in the expression, Eq. (16), as long as

$$\min_m \left(E_m^{N+2} - E_0^N\right) > 2\nu > \max_n \left(E_0^N - E_n^{N-2}\right),$$

such that the $N+2$ eigenvalues are positive and the $N-2$ eigenvalues are negative. A proper chemical potential also categorizes $\mathbf{M}$ to be positive definite, equivalent to the stability condition (see Subsection 3 in the Appendix for details).

III. PROOF OF THE EQUIVALENCE OF PP-RPA AND LADDER-CCD

The CCD ansatz, the simplest method in the coupled cluster family, expresses the wavefunction as

$$|\mathrm{CCD}\rangle = e^{\hat{T}_2}|\Phi_0\rangle, \tag{17}$$

where $|\Phi_0\rangle$ is a single Slater determinant, and $\hat{T}_2$ is the two-body cluster operator

$$\hat{T}_2 = \frac{1}{(2!)^2}\sum_{ijab} t_{ij}^{ab}\hat{a}^\dagger\hat{i}\hat{b}^\dagger\hat{j} = \sum_{ijab}^{i>j,a>b} t_{ij}^{ab}\hat{a}^\dagger\hat{i}\hat{b}^\dagger\hat{j}, \tag{18}$$

where $\hat{a}^\dagger$, $\hat{i}$ are the creation and annihilation operators for spin orbital a and i, respectively, and t_{ij}^{ab} is the double excitation amplitude, having the symmetry

$$t_{ij}^{ab} = -t_{ji}^{ab} = -t_{ij}^{ba} = t_{ji}^{ba}. \tag{19}$$

The correlation energy is expressed in terms of the amplitudes through the energy equation

$$E_c^{\mathrm{CCD}} = \sum_{ijab}^{i>j,a>b} \langle ij||ab\rangle t_{ij}^{ab}, \tag{20}$$

while the amplitudes t_{ij}^{ab} are solved by the CCD amplitude equation (see Ref. 52 for extensive discussions),

$$(\epsilon_i + \epsilon_j - \epsilon_a - \epsilon_b)t_{ij}^{ab}$$
$$= \langle ab||ij\rangle + \frac{1}{2}\sum_{cd}\langle ab||cd\rangle t_{ij}^{cd} + \frac{1}{2}\sum_{kl}\langle ij||kl\rangle t_{kl}^{ab}$$
$$-\sum_{kc}\left(\langle bk||cj\rangle t_{ik}^{ac} - \langle bk||ci\rangle t_{jk}^{ac} - \langle ak||cj\rangle t_{ik}^{bc} + \langle ak||ci\rangle t_{jk}^{bc}\right)$$
$$+\sum_{klcd}\langle kl||cd\rangle\left[\frac{1}{4}t_{ij}^{cd}t_{kl}^{ab} - \frac{1}{2}\left(t_{ij}^{ac}t_{kl}^{bd} + t_{ij}^{bd}t_{kl}^{ac}\right)\right.$$
$$\left.-\frac{1}{2}\left(t_{ik}^{ab}t_{jl}^{cd} + t_{ik}^{cd}t_{jl}^{ab}\right) + \left(t_{ik}^{ac}t_{jl}^{bd} + t_{ik}^{bd}t_{jl}^{ac}\right)\right]. \tag{21}$$

By allowing only particle-hole summations in Eq. (21), Scuseria *et al.*[46] have shown that the amplitude equation reduces to the ph-RPA equation with exchange, i.e., the time-dependent Hartree-Fock (TDHF) equation. Further eliminating the exchange terms in the two-electron integrals yields the conventional direct ph-RPA. Similarly, if we allow only summations of particle pairs and hole pairs, Eq. (21) becomes

$$\sum_{kl}(\epsilon_k + \epsilon_l)t_{kl}^{ab}\delta_{ki}\delta_{jl} - \sum_{cd}(\epsilon_c + \epsilon_d)t_{ij}^{cd}\delta_{ac}\delta_{bd}$$
$$= \langle ab||ij\rangle + \frac{1}{2}\sum_{cd}\langle ab||cd\rangle t_{ij}^{cd} + \frac{1}{2}\sum_{kl}\langle ij||kl\rangle t_{kl}^{ab}$$
$$+\frac{1}{4}\sum_{kl,cd} t_{kl}^{ab}\langle kl||cd\rangle t_{ij}^{cd}. \tag{22}$$

We refer to this truncated CCD as ladder-CCD, due to its restriction to ladder diagrams included in the correlation energy.[45] The exponential wavefunction of Eq. (17) with exponent of Eq. (27) has been proposed in Ref. 8, together with a similar form for ph-RPA, however without exploring their connection to the form of truncated CCD, a question worthwhile investigating, considering that there are several possibilities to evaluate the energy of an exponential wavefunction.[60] By utilizing the antisymmetry of the two-electron integrals $\langle uv||st\rangle = -\langle uv||ts\rangle$, Eq. (22) can be rearranged as

$$\sum_{cd}^{c>d} A_{ab,cd}t_{ij}^{cd} + \sum_{kl}^{k>l} C_{ij,kl}t_{kl}^{ab} + B_{ab,ij} + \sum_{kl,cd}^{k>l,c>d} t_{kl}^{ab}B_{cd,kl}^{*}t_{ij}^{cd} = 0, \tag{23}$$

with A, B, and C defined in Eqs. (2)–(4). Denoting the amplitude as a matrix $T_{ab,ij} = t_{ij}^{ab}$, Eq. (23) results in an algebraic matrix equation

$$\mathbf{AT} + \mathbf{TC} + \mathbf{B} + \mathbf{TB}^{\dagger}\mathbf{T} = 0. \quad (24)$$

Now, we will show that the pp-RPA equation of Eq. (1) is equivalent to the ladder-CCD amplitude equation under the assumption that the pp-RPA equation is stable.

The pp-RPA equation for only the $N + 2$ excitations reads,

$$\begin{bmatrix} \mathbf{A} & \mathbf{B} \\ \mathbf{B}^{\dagger} & \mathbf{C} \end{bmatrix} \begin{bmatrix} \mathbf{X} \\ \mathbf{Y} \end{bmatrix} = \begin{bmatrix} \mathbf{I} & \mathbf{0} \\ \mathbf{0} & -\mathbf{I} \end{bmatrix} \begin{bmatrix} \mathbf{X} \\ \mathbf{Y} \end{bmatrix} \boldsymbol{\omega}^{N+2}, \quad (25)$$

where $\dim \mathbf{X} = N_p \times N_p$, $\dim \mathbf{Y} = N_h \times N_p$, and $\dim \boldsymbol{\omega}^{N+2} = N_p \times N_p$. Multiplying $\mathbf{X}^{-1}$ from the right on Eq. (25) gives

$$\begin{bmatrix} \mathbf{A} & \mathbf{B} \\ \mathbf{B}^{\dagger} & \mathbf{C} \end{bmatrix} \begin{bmatrix} \mathbf{I} \\ \tilde{\mathbf{T}}^{\dagger} \end{bmatrix} = \begin{bmatrix} \mathbf{I} & \mathbf{0} \\ \mathbf{0} & -\mathbf{I} \end{bmatrix} \begin{bmatrix} \mathbf{I} \\ \tilde{\mathbf{T}}^{\dagger} \end{bmatrix} \mathbf{R}, \quad (26)$$

where

$$\tilde{\mathbf{T}} = (\mathbf{Y}\mathbf{X}^{-1})^{\dagger}, \quad (27)$$

and

$$\mathbf{R} = \mathbf{X}\boldsymbol{\omega}^{N+2}\mathbf{X}^{-1}. \quad (28)$$

The invertibility of $\mathbf{X}$ is guaranteed by a stable pp-RPA equation (see Subsection 4 in the Appendix for the detailed proof). Multiplying $[\tilde{\mathbf{T}}^{\dagger}\ \mathbf{1}]$ from the left, Eq. (26) becomes

$$\tilde{\mathbf{T}}^{\dagger}\mathbf{A} + \tilde{\mathbf{T}}^{\dagger}\mathbf{B}\tilde{\mathbf{T}}^{\dagger} + \mathbf{B}^{\dagger} + \mathbf{C}\tilde{\mathbf{T}}^{\dagger} = 0. \quad (29)$$

Comparing Eqs. (24) and (29), we infer that $\mathbf{T} = \tilde{\mathbf{T}}$.

The particle-particle block of Eq. (26) gives

$$\mathbf{A} + \mathbf{BT}^{\dagger} = \mathbf{R}. \quad (30)$$

Then, the ladder-CCD correlation energy of Eq. (20) can be expressed as

$$E_{\mathbf{c}}^{\mathbf{ladder-CCD}} = \mathrm{Tr}(\mathbf{B}^{\dagger}\mathbf{T}) = [\mathrm{Tr}(\mathbf{R} - \mathbf{A})]^* = \sum_m \omega_m^{N+2} - \mathrm{Tr}\mathbf{A}, \quad (31)$$

which is identical to the pp-RPA correlation energy in Eq. (16). From Eqs. (22)–(24), it is also clear that the chemical potential has no contribution because they cancel each other in the CCD equations through $\mathbf{AT} + \mathbf{TC}$.

Alternatively, one can also derive the equivalence using the $N - 2$ excitation eigenvectors with similar techniques. The resulting amplitude will be the same, while the correlation energy expression will be the second equation in Eq. (16). An alternative proof of equivalence can also be formulated using a Schur decomposition in analogy to Appendix 5 in Ref. 46.

In conclusion, the correlation energy from pp-RPA is equivalent to that of ladder-CCD, assuming that the pp-RPA equation is stable. The equivalence raises the question if the nonlinear ladder-CCD equations always converge to the unique solution of the linear pp-RPA equation system.

IV. NUMERICAL DEMONSTRATIONS

All coupled cluster and second-order Møller–Plesset perturbation theory (MP2) computations reported herein are performed in a locally modified version of CFOUR,[61] while pp-RPA is performed with QM4D.[62]

Concerning the algorithm, truncating the CCD equations to include only the ladder diagrams (Eq. (22)) can be seen as a small modification of the CCD equations or a small extension of the linearized CCD, also known as CEPA(0) (coupled electron pair approximation) or D-MBPT(∞),[52] amplitude equations. Note that the computationally most expensive term of coupled-cluster singles and doubles (CCSD), scaling as $N_{\mathrm{occ}}^2 N_{\mathrm{vir}}^4$, is the major part of the term quadratic in the amplitudes of Eq. (22). In terms of efficiency, the matrix multiplications necessary for solving the non-linear system of equations in standard coupled cluster algorithms are traded against the diagonalization in the pp-RPA algorithm, which, at the non-optimized stage of the code,[62] is significantly slower than solving the non-linear equations. However, the diagonalization has the indisputable advantage that the solution is unique, whereas the non-linear coupled cluster equations have multiple minima (most of them lacking any physical meaning), without *a priori* guarantee or check that the "correct" solution is found.[52]

All computations are carried out in the unrestricted Hartree-Fock (UHF) framework, but without breaking spatial symmetry. The correlation consistent basis sets of Dunning and co-workers[63,64] have been applied with cartesian d- and f- atomic-orbitals. The ladder-CCD amplitudes are found to converge essentially as fast (or with a couple of iterations less) than the corresponding CCSD equations.

All total energies of ladder-CCD and pp-RPA (see Table I) agree exceedingly well, the largest difference being 10^{-5} hartree, which is on the same order of magnitude as the difference in nuclear repulsion energy between the two programs and can have its origin in, e.g., integral screening (SCF and CC iteration convergence have been checked carefully). In terms of correlation energy, ladder-CCD captures between 43% (Be) and 80% (Ne) of CCSD, while the full CCD energy recovers about 99%. Note that MP2 has minimum and maximum values of 70% and 99% for the same systems. Furthermore, changing to a DFT reference leads to an increased (in absolute terms) correlation energy, with minimum/maximum values reaching 51 (54)% and 92 (95)% for B3LYP[65,66] (PBE[67]) orbitals. It is important to point out that the present pp-RPA@DFT is not equivalent to ladder-CCD with a DFT reference when following the usual practice in the coupled cluster community:[68,69] for pp-RPA@DFT, the molecular orbital energies are the eigenvalues of the Kohn-Sham Hamiltonian. However, the use of DFT orbitals in coupled cluster computations is considered as a "non-HF" reference wavefunction, for which the one-particle Hamiltonian is not diagonal and the corresponding terms can be accounted for, yielding results that are much closer to HF based computations.[70,71]

As a graphical illustration, Figure 1(a) shows the case of a dissociating cationic dimer (Ne_2^+), a typical probe for (de)localization error. We are using a spatial symmetry ($D_{\infty h}$) preserving unrestricted HF reference wavefunction for Ne_2^+, which corresponds to the ${}^2\Sigma_g$ ground state, as compared to F_2^+ the ground state of which is ${}^2\Pi_g$.[74] Again, the total energies of ladder-CCD and pp-RPA are identical to

TABLE I. Total energies of various methods. Geometries are taken from the G3 set.[72,73] The basis set is cc-pVTZ. All energies are in Hartree.

	HF	pp-RPA@HF	Ladder-CCD	pp-RPA@PBE	pp-RPA@B3LYP	MP2	CCD	CCSD
He	− 2.861154	− 2.885608	− 2.885608	− 2.889343	− 2.888504	− 2.894441	− 2.900328	− 2.900351
Li	− 7.432706	− 7.443903	− 7.443903	− 7.444664	− 7.444450	− 7.446781	− 7.449184	− 7.449243
Be	− 14.572875	− 14.598923	− 14.598923	− 14.605231	− 14.603533	− 14.614751	− 14.632242	− 14.632817
B	− 24.532104	− 24.566435	− 24.566436	− 24.575674	− 24.573063	− 24.584950	− 24.604746	− 24.605490
C	− 37.691663	− 37.746778	− 37.746778	− 37.760145	− 37.756583	− 37.769564	− 37.789208	− 37.789809
N	− 54.400883	− 54.482916	− 54.482916	− 54.500883	− 54.496235	− 54.509992	− 54.525553	− 54.525893
O	− 74.811910	− 74.933839	− 74.933839	− 74.959853	− 74.953384	− 74.969918	− 74.985506	− 74.986128
F	− 99.405657	− 99.576884	− 99.576884	− 99.611587	− 99.603292	− 99.622736	− 99.633484	− 99.634177
Ne	− 128.532010	− 128.760771	− 128.760771	− 128.804849	− 128.794546	− 128.816523	− 128.817814	− 128.818536
CH_4	− 40.213408	− 40.372051	− 40.372054	− 40.411910	− 40.402169	− 40.432266	− 40.452031	− 40.452991
H_2O	− 76.056687	− 76.266046	− 76.266049	− 76.318304	− 76.305731	− 76.336459	− 76.340863	− 76.342084
NH_3	− 56.217964	− 56.404439	− 56.404440	− 56.452289	− 56.440556	− 56.471921	− 56.483441	− 56.484474
CH_2O	− 113.910280	− 114.227562	− 114.227552	− 114.313824	− 114.293495	− 114.341669	− 114.347547	− 114.351726

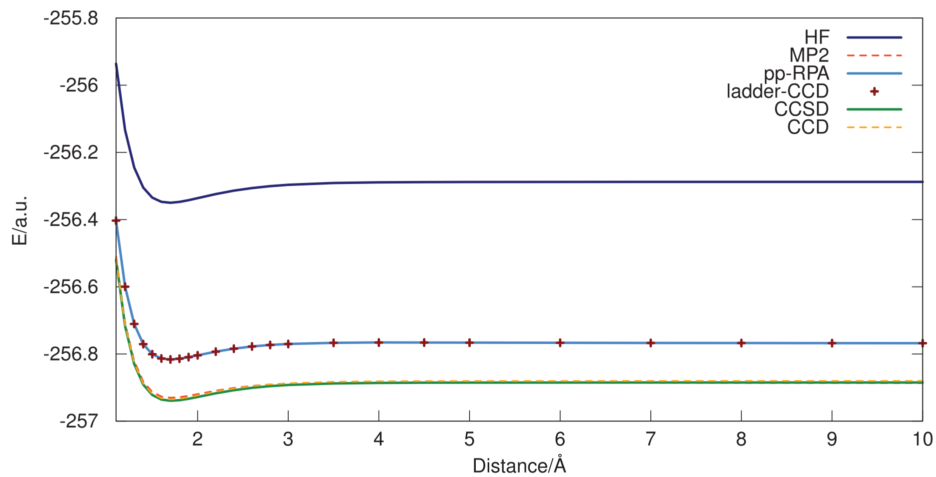

(a) The potential energy surface of Ne_2^+

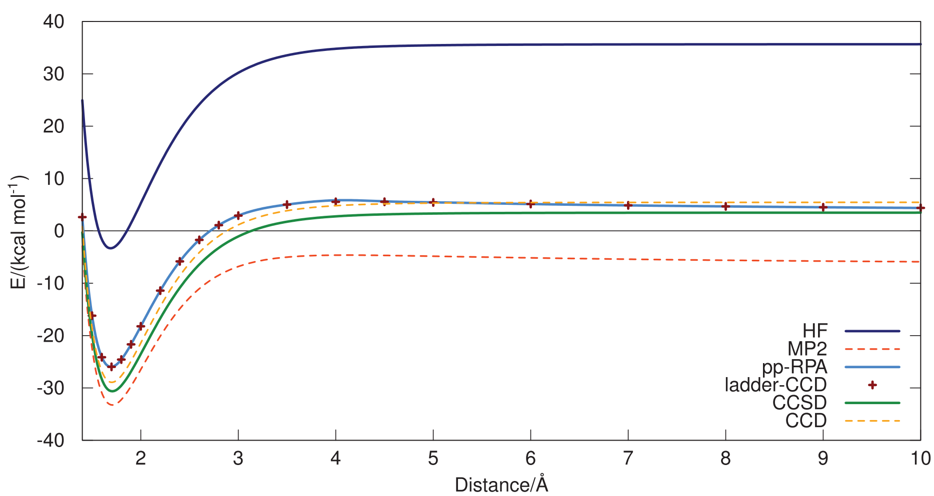

(b) The binding curve of Ne_2^+ (with respect to Ne and Ne^+)

FIG. 1. The potential energy surface (a) and the binding curve (b) of Ne_2^+ of various methods with the aug-cc-pVTZ basis set. The total energies of pp-RPA are substantially in error (a), since the correlation energy of the ladder diagrams is not very well balanced (MP2 total energies are, on the scale of the figure, indistinguishable from CCD, and pp-RPA is correct through second order[27]). However, the binding energy (b) reveals that the missing correlation energy cancels almost perfectly out, yielding a pp-RPA binding energy curve very close to CCD, while MP2 deviates from CCSD in the other direction (overbinding).

TABLE II. Atomization energies (in kcal mol^{-1}) of various methods. Geometries are taken from the G3 set.[72,73] Experimental atomization energies are taken from Refs. 76–79. The basis set is cc-pVTZ. The mean absolute deviation (MAD) is with respect to experimental data.

	HF	pp-RPA@HF	Ladder-CCD	pp-RPA@PBE	pp-RPA@B3LYP	MP2	CCD	CCSD	Expt.
CH_4	327.9	392.8	392.8	410.7	406.4	416.3	416.4	416.6	419.2
H_2O	153.8	208.7	208.7	225.8	221.7	230.3	223.2	223.6	232.2
NH_3	199.3	264.9	264.9	284.5	279.8	290.2	287.7	288.1	297.5
CH_2O	255.5	343.5	343.5	373.5	366.8	378.1	359.7	361.6	373.6
MAD	96.5	28.2	28.2	7.0	12.0	4.2	8.9	8.2	…

numerical precision (considering the two very different algorithms and programs), but not in very good agreement with CCSD. To further investigate the (de)localization error,[75] Figure 1(b) shows the binding energy with respect to the separated fragments. The binding energy of ladder-CCD is in fairly good agreement with CCSD and only a small "bump" is observed somewhere between 3 and 4 Å, revealing that the missing absolute correlation energies in ladder-CCD compared to CCSD are almost irrelevant for the binding energy. The localization error of HF is over-corrected by MP2, but increasing the correlation treatment to the coupled cluster level improves the dissociation limit further, leading to the previously reported[27] negligible fractional charge error.

Similarly to the binding energy of Ne_2^+, the atomization energies (Table II) illustrate that the correlation energy missing in ladder-CCD largely cancels out when computing reaction energies. For the four molecules considered, ladder-CCD provides 77% on of the correction between the HF and CCSD atomization energies on average. This is to be compared with MP2 which recovers on average 107%. However, the mean absolute deviation for pp-RPA@PBE compared to the experimental values is substantially better, having the same level of accuracy as CCSD.

In summary, the numerical analysis shows that ladder-CCD and pp-RPA are equivalent and that pp-RPA covers a substantial amount of correlation energy that is relevant for atomization energies of typical small molecules in Table II. An efficient pp-RPA implementation has, therefore, the potential to become a valuable electronic structure theory.

V. CONCLUSIONS

The connection between the linear pp-RPA equation and the quadratic ladder-CCD equation has been established and numerically verified. The numerical assessment suggests that pp-RPA is fairly accurate for some reaction energies, despite its incomplete diagram summation. This mathematical connection is helpful in establishing the relationship between Green's function based and the coupled-cluster methods. The ladder-CCD perspective of pp-RPA enables the straightforward study of its ground and excited state properties.

After finishing the development of Ref. 27 and this subsequent work, we became aware of independent research by Scuseria *et al.*[80] that follows the similar line of thought.

ACKNOWLEDGMENTS

Support from the Office of Naval Research (ONR) (N00014-09-1-0576) and the National Science Foundation (NSF) (CHE-09-11119) is gratefully appreciated. D.P. has also been supported by the William Krigbaum and Marcus Hobbs Fellowship from Duke University. S.N.S. acknowledges the Swiss NSF fellowship PBELP2_143559. H.v.A. appreciates the support form the FWO-Flanders (Scientific Research Fund Flanders). Discussions with Jianfeng Lu have been helpful.

APPENDIX: MATHEMATICAL ANALYSIS OF THE PP-RPA EQUATION

The Appendix discusses many mathematical properties of the pp-RPA equation. These properties are conceptually very similar to those of ph-RPA equation as shown in Ref. 10.

1. The zero signature of an eigenvector with an imaginary eigenvalue

For an eigenvalue ω_n and eigenvector $\mathbf{z}_n$, we have

$$\mathbf{M}\mathbf{z}_n = \omega_n \mathbf{W}\mathbf{z}_n. \tag{A1}$$

The Hermitian conjugate of Eq. (A1) becomes

$$\mathbf{z}_n^\dagger \mathbf{M} = \omega_n^* \mathbf{z}_n^\dagger \mathbf{W}. \tag{A2}$$

Multiplying $\mathbf{z}_n^\dagger$ to the left of Eq. (A1) and $\mathbf{z}_n$ to the right of Eq. (A2), we have

$$\mathbf{z}_n^\dagger \mathbf{M}\mathbf{z}_n = \omega_n \mathbf{z}_n^\dagger \mathbf{W}\mathbf{z}_n = \omega_n^* \mathbf{z}_n^\dagger \mathbf{W}\mathbf{z}_n.$$

Therefore,

$$(\omega_n - \omega_n^*)(\mathbf{z}_n^\dagger \mathbf{W}\mathbf{z}_n) = 0. \tag{A3}$$

For an imaginary eigenvalue $\omega_n \neq \omega_n^*$, the signature $\mathbf{z}_n^\dagger \mathbf{W}\mathbf{z}_n = 0$.

2. The orthonormalization of eigenvectors with all real eigenvalues

Using the same approach in Subsection 1 in the Appendix but with two different eigenvalues and eigenvectors, we have

$$\mathbf{z}_n^\dagger \mathbf{M}\mathbf{z}_m = \omega_m \mathbf{z}_n^\dagger \mathbf{W}\mathbf{z}_m = \omega_n^* \mathbf{z}_n^\dagger \mathbf{W}\mathbf{z}_m,$$

and

$$(\omega_m - \omega_n^*)(\mathbf{z}_n^\dagger \mathbf{W}\mathbf{z}_m) = 0. \tag{A4}$$

Therefore, when two real eigenvalues are different ($\omega_m \neq \omega_n^*$), the two eigenvectors are orthogonal under the metric $\mathbf{W}$ ($\mathbf{z}_n^\dagger \mathbf{W}\mathbf{z}_m = 0$). Since linear combination of eigenvectors of a degenerate eigenvalue stays in the same eigenspace, we can choose the eigenvectors of a degenerate eigenvalue to orthogonal to each other within the eigenspace. When all eigenvalues are real, eigenvectors can, therefore, be chosen to be orthogonalized under the metric $\mathbf{W}$. For a diagonalizable pp-RPA equation with all real eigenvalues, $\mathbf{z}_n^\dagger \mathbf{W} \mathbf{z}_n$ should not be zero, otherwise we have $\mathbf{z}_n^\dagger \mathbf{W} \mathbf{Z} = 0$, which indicates the eigenvector matrix is rank-deficit, which contradicts with the diagonalizability assumption. Therefore, the signatures of eigenvectors are all nonzero for a diagonalizable pp-RPA equation with all real eigenvalues. The resulting orthonormalization can be written as

$$\mathbf{Z}^\dagger \mathbf{W} \mathbf{Z} = \mathbf{\Lambda}, \tag{A5}$$

where Λ is a diagonal matrix with only ± 1 diagonal elements. According to Sylvester's law of inertia,[81] $\mathbf{W}$ and $\mathbf{\Lambda}$ share the same number of $+1$'s and -1's. In other words, there are N_{pp} $N+2$ excitations and N_{hh} $N-2$ excitations, according to the definition of $N \pm 2$ excitations in Sec. II. We can further arrange the eigenvectors such that eigenvectors with positive signatures stay in the left of $\mathbf{Z}$, then finally we reach the normalization condition

$$\mathbf{Z}^\dagger \mathbf{W} \mathbf{Z} = \mathbf{W}. \tag{A6}$$

3. The equivalence between stability and positive definiteness of M

First we show that the stability condition of Eq. (13) leads to the positive definiteness of $\mathbf{M}$.

From the stability of the pp-RPA equation (Eq. (13)) and the normalization (Eq. (12)), we have

$$\begin{aligned}
\mathbf{c}^\dagger \mathbf{M} \mathbf{c} &= \sum_{mn} (\mathbf{z}_m c_m)^\dagger \mathbf{M} (\mathbf{z}_n c_n) \\
&= \sum_{mn} c_m^* \mathbf{z}_m^\dagger \omega_n \mathbf{W} \mathbf{z}_n c_n \\
&= \sum_{n} c_m^* \delta_{mn} W_{mn} \omega_n c_n \\
&= \sum_{mn} c_m^* |\omega_m| \delta_{mn} c_n \\
&= \sum_{m} |c_m|^2 |\omega_m| > 0,
\end{aligned}$$

with an arbitrary nonzero column vector $\mathbf{c}$. Thus, $\mathbf{M}$ is positive definite for a pp-RPA equation.

Next, we show that the reverse is also true.

Given that $\mathbf{M}$ is positive definite, the pp-RPA equation in the compact form reads

$$\mathbf{M} \mathbf{z}_n = \omega_n \mathbf{W} \mathbf{z}_n. \tag{A7}$$

Since $\mathbf{M}$ is positive definite, Eq. (8) could be rewritten as

$$\mathbf{L}^\dagger \mathbf{z}_n = \omega_n \mathbf{L}^{-1} \mathbf{W} \left(\mathbf{L}^{-1}\right)^\dagger \mathbf{L}^\dagger \mathbf{z}_n,$$

where $\mathbf{M} = \mathbf{L}\mathbf{L}^\dagger$ is the Cholesky decomposition. With $\tilde{\mathbf{z}}_n = \mathbf{L}^\dagger \mathbf{z}_n$ and $\tilde{\mathbf{W}} = \mathbf{L}^{-1} \mathbf{W} (\mathbf{L}^{-1})^\dagger$, the eigenvalue problem

$$\tilde{\mathbf{W}} \tilde{\mathbf{z}}_n = \tilde{\omega}_n \tilde{\mathbf{z}}_n \tag{A8}$$

is diagonalizable with all real eigenvalues, since $\tilde{\mathbf{W}}^\dagger = \tilde{\mathbf{W}}$ by definition. Additionally, all eigenvalues of $\tilde{\mathbf{W}}$, $\tilde{\omega}_n$'s will be nonzero, since zero eigenvalue indicates $\det(\tilde{\mathbf{W}}) = 0$ which contradicts the definition of $\tilde{\mathbf{W}}$. With orthonormalization of the eigenvectors $\tilde{\mathbf{z}}_n^\dagger \tilde{\mathbf{z}}_m = \delta_{nm} |\tilde{\omega}_n|^{-1}$, Eq. (8) can be diagonalized with real eigenvalues

$$\omega_n = \tilde{\omega}_n^{-1}, \tag{A9}$$

and eigenvector orthonormalization with the eigenvalue sign constraints (the eigenvectors are arranged in the same way as in Subsection 2 in the Appendix),

$$\mathbf{z}_n^\dagger \mathbf{W} \mathbf{z}_m = \delta_{mn} \mathrm{sign}(\omega_m) = W_{nm}. \tag{A10}$$

Equation (A10) guarantees that the $\min_n \omega_n^{N+2} > 0 > \max_m \omega_m^{N-2}$. Therefore, by definition, this pp-RPA equation is stable, since all the eigenvalues are real and the $N+2$ and $N-2$ excitation spectra are nicely separated.

In summary, the stability condition of a pp-RPA equation is equivalent to the positive definiteness of $\mathbf{M}$.

4. The invertibility of X for a stable pp-RPA equation

We now prove the invertibility of $\mathbf{X}$ in Sec. III. According to Subsection 2 in the Appendix, the eigenvalues of a stable pp-RPA equation are orthonormalized according to

$$\mathbf{Z}^\dagger \mathbf{W} \mathbf{Z} = \mathbf{W}. \tag{A11}$$

For only $N+2$ excitation vectors,

$$\mathbf{Z}_{N+2}^\dagger \mathbf{W} \mathbf{Z}_{N+2} = \mathbf{I}, \tag{A12}$$

where

$$\mathbf{Z}_{N+2} = \begin{bmatrix} \mathbf{X} \\ \mathbf{Y} \end{bmatrix},$$

with $\mathbf{X}$ and $\mathbf{Y}$ the particle-particle and hole-hole block of the $N+2$ excitation eigenvector matrices. Expanding Eq. (A12), we have

$$\mathbf{X}^\dagger \mathbf{X} - \mathbf{Y}^\dagger \mathbf{Y} = \mathbf{I}. \tag{A13}$$

Therefore, $\mathbf{X}^\dagger \mathbf{X} = \mathbf{I} + \mathbf{Y}^\dagger \mathbf{Y}$ is positive definite, and $\mathbf{X}$ is invertible, otherwise $\mathbf{X}^\dagger \mathbf{X}$ will not be positive definite.

[1] D. Bohm and D. Pines, Phys. Rev. **82**, 625 (1951).
[2] D. Pines and D. Bohm, Phys. Rev. **85**, 338 (1952).
[3] J. Lindhard, K. Dan. Vidensk. Selsk. Mat. Fys. Medd. **28**, 8 (1954).
[4] A. G. Eguiluz, Phys. Rev. Lett. **51**, 1907 (1983).
[5] D. C. Langreth and J. P. Perdew, Solid State Commun. **17**, 1425 (1975).
[6] G. F. Giuliani and G. Vignale, *Quantum Theory of the Electron Liquid* (Cambridge University Press, 2005).
[7] J. Blaizot and G. Ripka, *Quantum Theory of Finite Systems* (Cambridge, MA, 1986).
[8] P. Ring and P. Schuck, *The Nuclear Many-Body Problem* (Springer, 2004).
[9] D. Thouless, Nucl. Phys. **21**, 225 (1960).
[10] D. D. Thouless, Nucl. Phys. **22**, 78 (1961).
[11] D. Thouless and J. Valatin, Nucl. Phys. **31**, 211 (1962).
[12] E. R. Marshalek and J. Weneser, Ann. Phys. **53**, 569 (1969).
[13] H. Eshuis, J. Yarkony, and F. Furche, J. Chem. Phys. **132**, 234114 (2010).
[14] F. Furche, J. Chem. Phys. **129**, 114105 (2008).
[15] S. Kurth and J. P. Perdew, Phys. Rev. B **59**, 10461 (1999).
[16] F. Furche, Phys. Rev. B **64**, 195120 (2001).

[17] M. Fuchs, Y.-M. Niquet, X. Gonze, and K. Burke, J. Chem. Phys. **122**, 94116 (2005).
[18] H. Eshuis and F. Furche, J. Chem. Phys. **136**, 84105 (2012).
[19] X. Ren, P. Rinke, C. Joas, and M. Scheffler, J. Mater. Sci. **47**, 7447 (2012).
[20] F. Furche and T. Van Voorhis, J. Chem. Phys. **122**, 164106 (2005).
[21] W. Zhu, J. Toulouse, A. Savin, and J. G. Angyán, J. Chem. Phys. **132**, 244108 (2010).
[22] J. Toulouse, W. Zhu, J. G. Ángyán, and A. Savin, Phys. Rev. A **82**, 032502 (2010).
[23] A. Hesselmann and A. Görling, Mol. Phys. **109**, 2473 (2011).
[24] M. Hellgren, D. R. Rohr, and E. K. U. Gross, J. Chem. Phys. **136**, 34106 (2012).
[25] P. Mori-Sánchez, A. J. Cohen, and W. Yang, Phys. Rev. A **85**, 42507 (2012).
[26] T. Gould and J. F. Dobson, J. Chem. Phys. **138**, 14109 (2013).
[27] H. van Aggelen, Y. Yang, and W. Yang, "Exchange-correlation energy from pairing matrix fluctuation and the particle-particle random phase approximation," preprint arXiv:1306.4957 (2013).
[28] O. Gunnarsson and B. Lundqvist, Phys. Rev. B **13**, 4274 (1976).
[29] N. Fukuda, F. Iwamoto, and K. Sawada, Phys. Rev. **135**, A932 (1964).
[30] J. Toivanen and J. Suhonen, Phys. Rev. Lett. **75**, 410 (1995).
[31] W. J. Mulhall, R. J. Liotta, J. A. Evans, and R. P. Perazzo, Nucl. Phys. A **93**, 261 (1967).
[32] D. J. Rowe, Phys. Rev. **175**, 1283 (1968).
[33] D. J. Rowe, Rev. Mod. Phys. **40**, 153 (1968).
[34] G. Ripka and R. Padjen, Nucl. Phys. A **132**, 489 (1969).
[35] J. Vary and J. N. Ginocchio, Nucl. Phys. A **166**, 479 (1971).
[36] G. Blanchon, N. V. Mau, A. Bonaccorso, M. Dupuis, and N. Pillet, Phys. Rev. C **82**, 34313 (2010).
[37] J. C. Pacheco and N. Vinh Mau, Phys. Rev. C **65**, 44004 (2002).
[38] K. A. Brueckner and C. A. Levinson, Phys. Rev. **97**, 1344 (1955).
[39] R. Eden, Proc. R. Soc. London, Ser. A **235**, 408 (1956).
[40] H. Bethe, Phys. Rev. **103**, 1353 (1956).
[41] J. Goldstone, Proc. R. Soc. London, Ser. A **239**, 267 (1957).
[42] C.-M. Liegener, J. Chem. Phys. **104**, 2940 (1996).
[43] C.-M. Liegener, Chem. Phys. Lett. **90**, 188 (1982).
[44] M. Gell-Mann and K. Brueckner, Phys. Rev. **106**, 364 (1957).
[45] J. Čížek, J. Chem. Phys. **45**, 4256 (1966).
[46] G. E. Scuseria, T. M. Henderson, and D. C. Sorensen, J. Chem. Phys. **129**, 231101 (2008).
[47] E. Sanderson, Phys. Lett. **19**, 141 (1965).
[48] R. F. Bishop, W. Piechocki, and G. A. Stevens, Few-Body Syst. **4**, 161 (1988).
[49] M. Nooijen and R. J. Bartlett, J. Chem. Phys. **102**, 3629 (1995).
[50] M. Nooijen and R. J. Bartlett, J. Chem. Phys. **106**, 6441 (1997).
[51] S. R. Gwaltney, R. J. Bartlett, and M. Nooijen, J. Chem. Phys. **111**, 58 (1999).
[52] I. Shavitt and R. J. Bartlett, *Many-Body Methods in Chemistry and Physics: MBPT and Coupled-Cluster Theory* (Cambridge University Press, 2009).
[53] H. Sekino and R. J. Bartlett, Int. J. Quantum Chem. **26**, 255 (1984).
[54] K. Kowalski, J. R. Hammond, and W. A. de Jong, J. Chem. Phys. **127**, 164105 (2007).
[55] M. E. Casida, in *Recent Advances in Computational Chemistry*, edited by D. P. Chong (World Scientific, Singapore, 1995), Vol. 1, p. 155.
[56] N. J. Higham, *Functions of Matrices: Theory and Computation*, SIAM e-books (Society for Industrial and Applied Mathematics (SIAM), Philadelphia, 2008).
[57] R. G. Parr and W. Yang, *Density-Functional Theory of Atoms and Molecules* (Oxford University Press, New York, 1989).
[58] W. H. Adams, Phys. Rev. **127**, 1650 (1962).
[59] D. Dehareng and G. Dive, J. Comput. Chem. **21**, 483 (2000).
[60] W. Kutzelnigg, Theor. Chim. Acta **80**, 349 (1991).
[61] CFOUR, Coupled-Cluster techniques for Computational Chemistry, a quantum-chemical program package by J. F. Stanton, J. Gauss, M. E. Harding, P. G. Szalay with contributions from A. A. Auer, R. J. Bartlett, U. Benedikt, C. Berger, D. E. Bernholdt, Y. J. Bomble, L. Cheng, O. Christiansen, M. Heckert, O. Heun, C. Huber, T.-C. Jagau, D. Jonsson, J. Juselius, K. Klein, W. J. Lauderdale, D. A. Matthews, T. Metzroth, L. A. Muck, D. P. O'Neill, D. R. Price, E. Prochnow, C. Puzzarini, K. Ruud, F. Schiffmann, W. Schwalbach, S. Stopkowicz, A. Tajti, J. Vazquez, F. Wang, J. D. Watts and the integral packages MOLECULE (J. Almlof and P. R. Taylor), PROPS (P. R. Taylor), ABACUS (T. Helgaker, H. J. Aa. Jensen, P. Jorgensen, and J. Olsen), and ECP routines by A. V. Mitin and C. van Wullen, see http://www.cfour.de for the current version.
[62] An in-house program for QM/MM simulations, see http://www.qm4d.info.
[63] T. H. Dunning, J. Chem. Phys. **90**, 1007 (1989).
[64] D. E. Woon and T. H. Dunning, J. Chem. Phys. **98**, 1358 (1993).
[65] A. D. Becke, J. Chem. Phys. **98**, 5648 (1993).
[66] C. T. Lee, W. T. Yang, and R. G. Parr, Phys. Rev. B **37**, 785 (1988).
[67] J. P. Perdew, K. Burke, and M. Ernzerhof, Phys. Rev. Lett. **77**, 3865 (1996).
[68] R. J. Bartlett, I. Grabowski, S. Hirata, and S. Ivanov, J. Chem. Phys. **122**, 34104 (2005).
[69] R. J. Bartlett, V. F. Lotrich, and I. V. Schweigert, J. Chem. Phys. **123**, 62205 (2005).
[70] J. D. Watts, J. Gauss, and R. J. Bartlett, J. Chem. Phys. **98**, 8718 (1993).
[71] G. J. O. Beran, S. R. Gwaltney, and M. Head-Gordon, Phys. Chem. Chem. Phys. **5**, 2488 (2003).
[72] L. A. Curtiss, K. Raghavachari, P. C. Redfern, and J. A. Pople, J. Chem. Phys. **112**, 7374 (2000).
[73] L. A. Curtiss, P. C. Redfern, and K. Raghavachari, J. Chem. Phys. **123**, 124107 (2005).
[74] J. D. Watts and R. J. Bartlett, J. Chem. Phys. **95**, 6652 (1991).
[75] P. Mori-Sánchez, A. Cohen, and W. Yang, Phys. Rev. Lett. **100**, 146401 (2008).
[76] J. A. Pople, M. Head-Gordon, D. J. Fox, K. Raghavachari, and L. A. Curtiss, J. Chem. Phys. **90**, 5622 (1989).
[77] L. A. Curtiss, C. Jones, G. W. Trucks, K. Raghavachari, and J. A. Pople, J. Chem. Phys. **93**, 2537 (1990).
[78] L. A. Curtiss, K. Raghavachari, P. C. Redfern, and J. A. Pople, J. Chem. Phys. **106**, 1063 (1997).
[79] C. Adamo, M. Ernzerhof, and G. E. Scuseria, J. Chem. Phys. **112**, 2643 (2000).
[80] G. E. Scuseria, T. M. Henderson, and I. W. Bulik, J. Chem. Phys. **139**, 104113 (2013).
[81] R. A. Horn and C. R. Johnson, *Matrix Analysis* (Cambridge University Press, 1990).
[82] J. V. Ortiz, J. Chem. Phys. **81**, 5873 (1984).